Roles of the Two *Drosophila* CRYPTOCHROME Structural Domains in Circadian Photoreception

Ania Busza,[1]* Myai Emery-Le,[1]* Michael Rosbash,[2] Patrick Emery[1]†

CRYPTOCHROME (CRY) is the primary circadian photoreceptor in *Drosophila*. We show that CRY binding to TIMELESS (TIM) is light-dependent in flies and irreversibly commits TIM to proteasomal degradation. In contrast, CRY degradation is dependent on continuous light exposure, indicating that the CRY-TIM interaction is transient. A novel *cry* mutation (*cry^m*) reveals that CRY's photolyase homology domain is sufficient for light detection and phototransduction, whereas the carboxyl-terminal domain regulates CRY stability, CRY-TIM interaction, and circadian photosensitivity. This contrasts with the function of *Arabidopsis* CRY domains and demonstrates that insect and plant cryptochromes use different mechanisms.

Cyanobacteria and eukaryotes adapt to the daily physical and ecological changes in their environment with the help of circadian pacemakers. In most organisms, these pacemakers are based on a 24-hour period transcriptional negative feedback loop (*1*). In *Drosophila melanogaster*, PERIOD (PER) and TIMELESS (TIM) dimerize and function as negative transcription factors by interfering with the positive activity of CLOCK (CLK) and CYCLE (CYC), which together bind to and activate the *per* and *tim* promoters (*2*). A set of kinases (SHAGGY, DOUBLETIME, and CASEIN KINASE-II) regulates PER and TIM stability and activity to ensure that the cycle lasts 24 hours (*2–4*).

Circadian pacemakers require input pathways to synchronize with the environment. Cryptochromes are blue light–sensitive proteins related to photolyases, a family of DNA repair enzymes. They play important roles in plants and animal circadian photoreception (*5*). There is good evidence that *Drosophila* CRYPTOCHROME (CRY) is the primary circadian photoreceptor, although opsin photoreception also helps to synchronize circadian behavior (*6*). CRY overexpression increases the sensitivity of the circadian clock, and all circadian photoresponses are affected in the severely hypomorphic *cry^b* mutant (*7–10*). However, the mechanisms by which CRY synchronizes the circadian pacemaker are still unclear. The primary target of the CRY input pathway appears to be TIM. TIM light-dependent degradation requires CRY and is crucial to reset the circadian pacemaker after short light pulses (*9*, *11–16*). Both CRY and TIM are degraded by the proteasome after illumination (*17*, *18*), and they interact in a light-dependent manner in yeast (*19*). In *Drosophila* S2 cells, however, the CRY-TIM interaction is apparently light-independent (*19*). Moreover, CRY interacts with PER, which suggests that PER might also be a pacemaker target of CRY. Like TIM, PER undergoes a light-dependent interaction with CRY in yeast but interacts with CRY in the dark in S2 cells (*20*).

To study CRY and its interactions directly in flies, we generated flies expressing an N-terminal MYC-tagged CRY (*y w; tim-GAL4 UAS-myccry/CyO*) (*tmc* flies). MYC-CRY is fully functional, as it rescues PER and TIM cycling and arrhythmic constant-light behavior in *cry^b* flies (*21*). *tmc* and *y w* control flies were light-pulsed for 15 min in the late night when PER and TIM levels are high [zeitgeber time (ZT) 21], and CRY binding to PER and TIM was assayed by immunoprecipitation with antibody to MYC. A strong light-dependent interaction was evident among CRY, TIM, and PER (Fig. 1A), and comparable results were observed at earlier times, at ZT 15 and ZT 17 (*21*). A weak TIM and PER signal was visible in the dark, but a comparable background signal was visible in *y w* control flies, indicating that there is no detectable binding of CRY to PER and TIM in the dark. Thus, if CRY interacts with PER and TIM in the dark as previously suggested (*19*, *20*), it might be limited to the specific tissues in which CRY contributes to circadian oscillations in constant conditions (*22*, *23*).

Because TIM and PER interact strongly, we examined whether CRY binds to TIM or PER individually. We clearly detected a light-dependent CRY-TIM interaction in *per^0* flies (Fig. 1B). Similar results were obtained in S2 cells (Fig. 1C), in contrast to a previous report (*19*, *24*). These findings, together with the original yeast data (*19*), imply that the CRY-TIM light-sensitive interaction occurs in all expression systems. We failed to detect any interaction between CRY and PER without TIM, either in *tim^0* flies or in S2 cells (*21*, *24*); thus, TIM appears to be CRY's primary target after light activation. The PER immunoprecipitation from wild-type flies reflects the strong PER-TIM interaction.

To understand the consequences of the TIM-CRY interaction, we assayed TIM and CRY degradation kinetics after light exposure (Fig. 2A). We first expressed CRY alone in S2 cells and monitored its degradation. CRY was very stable in the dark but rapidly degraded in the light, with a half-life of about 25 min. However, after 10 min of light exposure and then 50 min of darkness, CRY levels were only slightly lower than after the 10-min light pulse and much

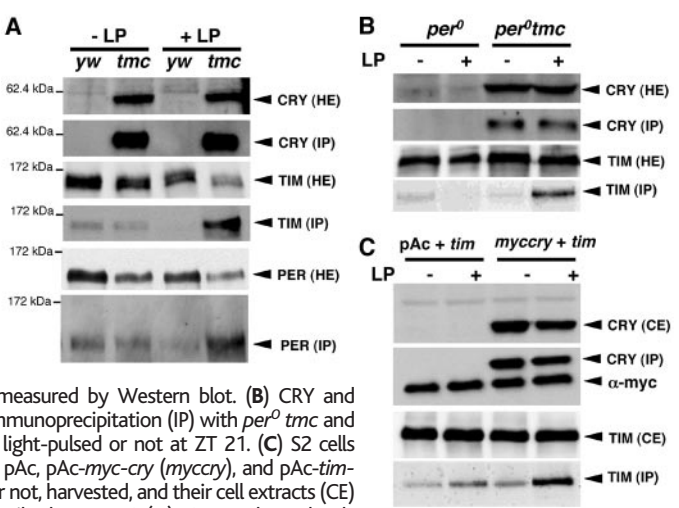

Fig. 1. Light-dependent interactions among CRY, TIM, and PER in vivo and in S2 cells. (**A**) *tmc* flies (see text) and *y w* control flies were subjected to light:dark conditions, light-pulsed (LP) or not for 15 min at ZT 21 (lights are turned on at ZT 0 and turned off at ZT 12), collected, and frozen. Head extracts (HE) were immunoprecipitated with antibody to MYC (IP), and CRY, TIM, and PER levels were measured by Western blot. (**B**) CRY and TIM levels after anti-MYC immunoprecipitation (IP) with *per^0 tmc* and *per^0* fly head extracts (HE) light-pulsed or not at ZT 21. (**C**) S2 cells transiently transfected with pAc, pAc-*myc-cry* (*myccry*), and pAc-*tim-HA* (*tim*) were light-pulsed or not, harvested, and their cell extracts (CE) immunoprecipitated with antibody to MYC (IP). CRY and TIM levels were measured by Western blot.

[1]Department of Neurobiology, University of Massachusetts Medical School, 364 Plantation Street, Worcester, MA 01605, USA. [2]Howard Hughes Medical Institute, Brandeis University, 415 South Street, Waltham, MA 02454, USA.

*These authors contributed equally to this work.
†To whom correspondence should be addressed. E-mail: patrick.emery@umassmed.edu

higher than after the 60-min light pulse [Fig. 2A, left; the difference in the number of photons delivered with the different light protocols does not account for these results (*24*)]. The same phenomenon was observed in vivo (Fig. 2A, center) in the presence of PER and TIM. CRY degradation therefore requires continuous light exposure, and CRY can rapidly revert to a stable conformation when returned to darkness. We then assayed TIM after light exposure in wild-type flies. The TIM degradation time course was virtually indistinguishable from that of CRY, with a half-life of 20 min. However, the 10-min light pulse plus 50-min dark protocol produced TIM levels close to those seen after a 60-min light pulse (Fig. 2A, right). A 10-min light pulse therefore commits TIM, but not CRY, to degradation. This finding indicates that different mechanisms govern TIM and CRY degradation and suggests that the two proteins interact transiently.

To strengthen the notion that TIM and CRY interact after CRY absorbs light, we measured the wavelength sensitivity of CRY in S2 cells, using its own light-dependent degradation as a readout. Previous experiments in flies have shown that the spectral sensitivity of TIM's light-dependent degradation closely matches the spectral sensitivity for behavioral phase resetting. Maximal effects are observed between 400 and 500 nm, and virtually no response is detected above 550 nm (Fig. 2B) (*15*). The spectral sensitivity of CRY degradation in S2 cells (Fig. 2B) is remarkably consistent with the two previous spectral sensitivities in flies. This result strongly reinforces the notion that CRY is the primary photoreceptor for TIM degradation and phase resetting.

CRY contains a photolyase homology domain and a C-terminal domain, like most cryptochrome family members (fig. S2) (*5*). To determine the contribution of these two domains, we studied a *cry* variant isolated in a novel genetic screen for mutants remaining rhythmic in constant 3000-lux light. Wild-type *Drosophila* circadian period lengthens under constant low light intensity (<10 lux), but flies are arrhythmic at higher intensities (*25*). In contrast, cry^b flies maintain robust ~24-hour rhythms even in intense constant light (*8*). We isolated a rhythmic mutant line with a period slightly longer than 24 hours under constant light. [In constant darkness, both the mutant and the parental strain also showed a slightly long circadian period (Fig. 3A) (table S1).] The new mutant failed to complement the cry^b constant-light defect, which indicated that the new mutation was in *cry* (Fig. 3A). This new *cry* allele, which we named cry^m, contains a single change from the wild-type line used for the mutagenesis: a premature stop codon that truncates CRY's last 19 amino acids, leaving the photolyase domain intact (fig. S2).

To understand how the loss of CRY's C-terminal domain so profoundly affects constant-light behavior, we measured CRY^M levels in fly heads (Fig. 3B, top). Weak bands were visible, at the position of CRY and just below, which might correspond to the truncated CRY^M protein. Mutant protein levels appeared lower than those of cry^b flies. When expressed in S2 cells, CRY^M was clearly visible, but at levels lower than those of wild-type CRY by a factor of at least 20 (Fig. 3B, bottom). A 2-hour light pulse did not noticeably change CRY^M levels. However, addition of the proteasome inhibitor MG-132 strongly increased CRY^M and CRY^B stability (Fig. 3C). Because MG-132 also inhibits CRY light-dependent degradation (*17*), the data show that both mutant proteins are constitutively degraded by the proteasome, rather than being degraded in a light-dependent manner.

These results suggest that cry^m flies, like cry^b flies, are blind to constant light because the CRY^M protein is unstable and nonfunctional. However, exposure of cry^m flies to lower constant-light intensities lengthened the circadian period: At 200 lux, the cry^m period lengthened to 25.1 hours. It lengthened even further to 26.6 hours at 25 lux (table S1) (*24*). (cry^b flies were unaffected under identical conditions.) This behavior of cry^m flies indicates that their circadian clock is not blind and that the CRY^M protein provides light signal to the pacemaker. This is possibly because CRY^M can accumulate to slightly higher levels under low light intensity in the neurons controlling circadian behavior (*24*).

We then measured other CRY-dependent circadian photoresponses in cry^m flies. In whole head extracts, most PER and TIM signals come from the eyes, a tissue with no detectable circadian oscillations in cry^b flies under light:dark conditions. In contrast, PER and TIM oscillations were clearly present in cry^m flies, although the amplitude was reduced relative to wild-type flies (Fig. 4A). We then tested the effect of the cry^m mutation on the ability of the circadian pacemaker to respond to short light pulses. We briefly illuminated wild-type, cry^b, and cry^m flies at different times of the night and determined the effect on circadian behavioral phase (Fig. 4B). For wild-type flies, as expected, there were phase delays in the early night and phase advances in the late night. cry^b flies showed little or no responses, whereas cry^m flies were still able to advance or delay their clock but with a reduced magnitude. Be-

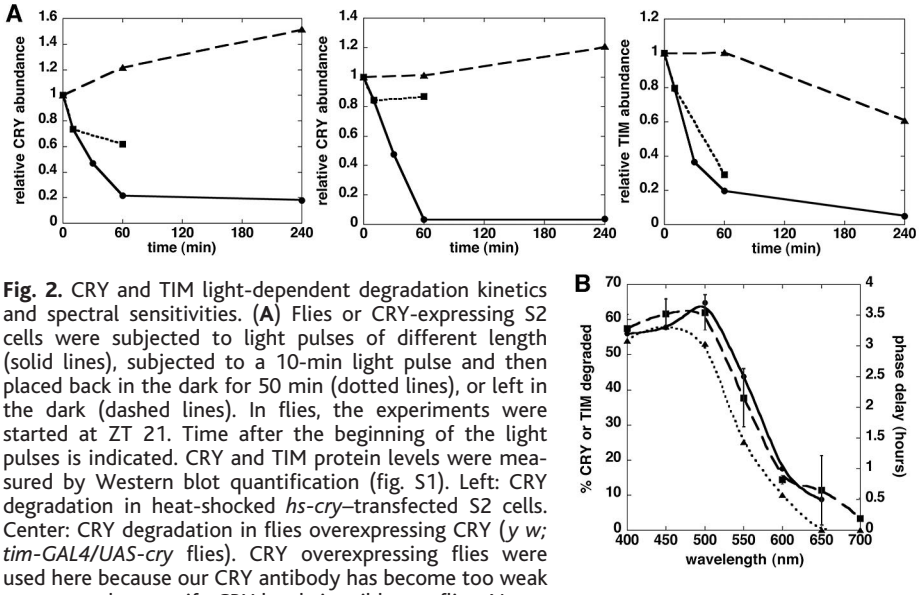

Fig. 2. CRY and TIM light-dependent degradation kinetics and spectral sensitivities. (**A**) Flies or CRY-expressing S2 cells were subjected to light pulses of different length (solid lines), subjected to a 10-min light pulse and then placed back in the dark for 50 min (dotted lines), or left in the dark (dashed lines). In flies, the experiments were started at ZT 21. Time after the beginning of the light pulses is indicated. CRY and TIM protein levels were measured by Western blot quantification (fig. S1). Left: CRY degradation in heat-shocked *hs-cry*–transfected S2 cells. Center: CRY degradation in flies overexpressing CRY (*y w; tim-GAL4/UAS-cry* flies). CRY overexpressing flies were used here because our CRY antibody has become too weak to accurately quantify CRY levels in wild-type flies. Nonetheless, the qualitative results observed in wild-type flies were similar (*21*). Right: TIM degradation in wild-type (*y w*) flies. These experiments were reproduced with similar results. (**B**) Spectral sensitivity of CRY light-dependent degradation in S2 cells at an irradiance of 2.5×10^{17} photons cm^{-2} s^{-1} (dashed line). Heat-shocked *hs-cry*–transfected cells were pulsed for 1 hour with monochromatic lights of different colors. CRY levels after the pulse were determined by Western blot quantification and compared with the levels obtained in cells that were not pulsed. Data are averages of three independent experiments; SDs are shown. The left *y* axis indicates the percentage of CRY degraded after the pulse; the *x* axis indicates the wavelength of the monochromatic light. The spectral sensitivities of TIM degradation (dotted line) (*15*) and of behavioral phase response to short light pulse at ZT 15 (solid line) (*15*) are also shown. The left *y* axis also indicates the percentage of TIM degraded after a light pulse, and the right *y* axis the phase change in hours after a short light pulse at ZT 15.

cause we had observed that cry^m flies detect constant light better at low intensity, we reduced the intensity of the light:dark regime to 25 lux instead of 1000 lux. The intensity of the light pulses was unchanged (3000 lux). The results were striking, as the magnitude of the cry^m phase changes was almost as robust as that of wild-type flies (Fig. 4C). In contrast, the low-intensity regime had no effect on the cry^b responses, confirming previous studies showing that cry^b is a null allele, or nearly so (*8*–*10*, *19*). These results indicate that the CRY^M protein is fully functional for circadian phototransduction, despite the absence of the C-terminal domain.

In support of our conclusions, we found that CRY^M can bind TIM as strongly as wild-type CRY can (fig. S3). This is also true for CRY^B. However, CRY^M and CRY^B bind TIM equally well in the dark or after a light pulse, whereas wild-type CRY binds TIM only when light is present. The mutant proteins cannot bind PER, which indicates that they retain specificity for TIM (*21*). These results suggest that there are two separable consequences of CRY photon capture that induce circadian photoresponses. The first is CRY binding to TIM, which is presumably necessary but not sufficient for signal transduction. The second is the irreversible modification of TIM for its targeting to proteasomal degradation, probably with the help of a tyrosine kinase (*18*). CRY^M can achieve the second step because its photolyase domain is unaltered and sensitive to light. CRY^B fails to trigger light-dependent TIM degradation because its mutation probably results in an inability to bind flavin adenine dinucleotide properly (fig. S2) (*9*). We interpret the failure of CRY^B to act as a dominant negative mutant as a consequence of its low expression level.

In sum, we propose that CRY's photolyase domain is fully responsible for phototransduction and that the C-terminal domain is not required for this activity. In contrast, the C-terminal domain inhibits the CRY-TIM interaction in the dark and determines the photosensitivity of the circadian clock by regulating CRY proteasomal degradation. This view of CRY photoreception in *Drosophila* contrasts sharply with what we know about *Arabidopsis thaliana* CRYs: In these molecules, the C terminus is the active phototransduction domain, and the photolyase region modulates its signaling function (*26*). Strikingly different mechanistic strategies have therefore emerged during evolution to transmit light information and regulate CRY activity. Interestingly, *Drosophila* TIM is related to molecules involved in various aspects of DNA metabolism—including chromosome segregation and DNA repair—in various organisms (*27*–*31*). The CRY-TIM interaction, mediated by the DNA-repair photolyase homology domain, may thus be evolutionarily ancient and may have been central to the origin of circadian rhythms.

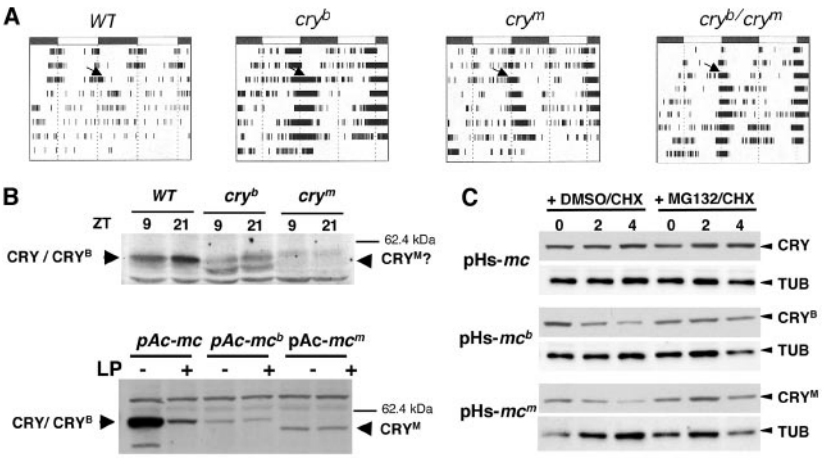

Fig. 3. Isolation of a new *cry* variant: cry^m. (**A**) Representative actograms for wild-type (Canton-S strain, *WT*), cry^b, cry^m, and heterozygous cry^m/cry^b flies. Flies were subjected to a light:dark cycle for 3 days and then left under constant light. The arrows indicate when the lights were left on instead of being turned off. (**B**) Top: CRY protein levels in wild-type (Canton-S, *WT*), cry^b, and cry^m flies measured by Western blot. Flies were kept under light:dark conditions. Flies were collected at the indicated ZTs. CRY^M levels are very low, and the band corresponding to CRY^M could not be identified with certainty. Bottom: CRY, CRY^B, and CRY^M protein levels in S2 cells transfected with pAc-*myccry* (*pAc-mc*), pAc-$myccry^b$ (*pAc-*mc^b), and pAc-$myccry^m$ (*pAc-*mc^m) vectors, light-pulsed (+) or not (–) for 2 hours. (**C**) CRY, CRY^B, and CRY^M protein levels in heat-shocked S2 cells transfected with pHS-*myccry*, pHS-$myccry^b$, and pHS-$myccry^m$ vectors and treated with 50 μM MG132 diluted in dimethyl sulfoxide (DMSO), or with DMSO only. All transfected cells were also treated with cycloheximide (0.5 mg/ml) to block protein synthesis. The drugs were added 2 hours after the heat shock. Time after addition of the drug is indicated in hours. α-Tubulin (TUB) levels were used as loading control. Similar results were obtained when CRY, CRY^B, and CRY^M were expressed with the constitutive actin promoter [pAc vectors (*21*)]. Antibodies to CRY [(B), top] and to MYC [(B), bottom, and (C)] were used for the Western blots.

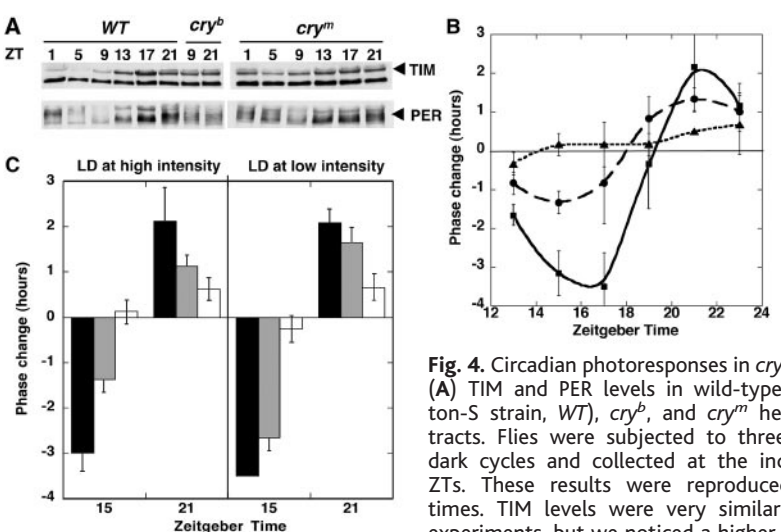

Fig. 4. Circadian photoresponses in cry^m flies. (**A**) TIM and PER levels in wild-type (Canton-S strain, *WT*), cry^b, and cry^m head extracts. Flies were subjected to three light:dark cycles and collected at the indicated ZTs. These results were reproduced four times. TIM levels were very similar in all experiments, but we noticed a higher degree of variability in PER levels in cry^m flies. (**B**) Phase response curve for wild-type (Canton-S strain, *WT*, solid line), cry^b (dotted line), and cry^m flies (dashed line). Flies were entrained under a 12-hour light:12-hour dark regime. The light intensity during the day was 1000 lux. The flies were then pulsed during the last night of the light:dark regime at 3000 lux for 5 min, and then left in constant darkness. Their phase was compared to those of flies that had not been pulsed. Phase change is plotted on the *y* axis; phase delays and advances are shown as negative and positive values, respectively. The *x* axis represents the ZT of the light pulse. Data are averages of four independent experiments; SDs are shown. (**C**) The responses to short 3000-lux light pulses were measured at ZTs 15 and 21 in wild-type (Canton-S strain, *WT*, black bars), cry^m (gray bars), and cry^b flies (white bars) exposed to a light:dark regime (LD) with high (1000 lux, left) or low (25 lux, right) light intensities. The *x* and *y* axes are as in (B). Data are averages of three independent experiments; SDs are shown.

References and Notes

1. J. C. Dunlap, *Cell* **96**, 271 (1999).
2. R. Stanewsky, *Cell Tissue Res.* **309**, 11 (2002).
3. J. M. Lin *et al.*, *Nature* **420**, 816 (2002).
4. B. Akten *et al.*, *Nature Neurosci.* **6**, 251 (2003).
5. A. R. Cashmore, *Cell* **114**, 537 (2003).
6. C. Helfrich-Forster, C. Winter, A. Hofbauer, J. C. Hall, R. Stanewsky, *Neuron* **30**, 249 (2001).
7. P. Emery, W. V. So, M. Kaneko, J. C. Hall, M. Rosbash, *Cell* **95**, 669 (1998).
8. P. Emery, R. Stanewsky, J. C. Hall, M. Rosbash, *Nature* **404**, 456 (2000).
9. R. Stanewsky *et al.*, *Cell* **95**, 681 (1998).
10. P. Emery *et al.*, *Neuron* **26**, 493 (2000).
11. M. Hunter-Ensor, A. Ousley, A. Sehgal, *Cell* **84**, 677 (1996).
12. C. Lee, V. Parikh, T. Itsukaichi, K. Bae, I. Edery, *Science* **271**, 1740 (1996).
13. M. P. Myers, K. Wager-Smith, A. Rothenfluh-Hilfiker, M. W. Young, *Science* **271**, 1736 (1996).
14. H. Zeng, Z. Qian, M. P. Myers, M. Rosbash, *Nature* **380**, 129 (1996).
15. V. Suri, Z. Qian, J. C. Hall, M. Rosbash, *Neuron* **21**, 225 (1998).
16. Z. Yang, M. Emerson, H. S. Su, A. Sehgal, *Neuron* **21**, 215 (1998).
17. F. J. Lin, W. Song, E. Meyer-Bernstein, N. Naidoo, A. Sehgal, *Mol. Cell. Biol.* **21**, 7287 (2001).
18. N. Naidoo, W. Song, M. Hunter-Ensor, A. Sehgal, *Science* **285**, 1737 (1999).
19. M. F. Ceriani *et al.*, *Science* **285**, 553 (1999).
20. E. Rosato *et al.*, *Curr. Biol.* **11**, 909 (2001).
21. A. Busza, M. Emery-Le, M. Rosbash, P. Emery, data not shown.
22. M. Ivanchenko, R. Stanewsky, J. M. Giebultowicz, *J. Biol. Rhythms* **16**, 205 (2001).
23. B. Krishnan *et al.*, *Nature* **411**, 313 (2001).
24. See supporting data on *Science* Online.
25. R. J. Konopka, C. Pittendrigh, D. Orr, *J. Neurogenet.* **6**, 1 (1989).
26. H. Q. Yang *et al.*, *Cell* **103**, 815 (2000).
27. R. C. Chan *et al.*, *Nature* **424**, 1002 (2003).
28. E. Noguchi, C. Noguchi, L. L. Du, P. Russell, *Mol. Cell. Biol.* **23**, 7861 (2003).
29. H. Park, R. Sternglanz, *Yeast* **15**, 35 (1999).
30. Y. Katou *et al.*, *Nature* **424**, 1078 (2003).
31. E. J. Foss, *Genetics* **157**, 567 (2001).

32. We thank A. Murad for help with real-time PCR; V. Suri for the pAc-*per* vector; R. Allada for the pAc-*timha* vector; E. Rosato, S. Waddell, and S. M. Reppert for critical reading of our manuscript; and J. Levine, R. Stanewsky, and members of our labs for helpful discussions and suggestions. Supported by a Young Investigator Award from the Richard and Susan Smith Family Foundation and NIH grant GM66777-01 (P.E.), NIH Cellular and Molecular Neurobiology training grant 5 T32 NS07366-08 (A.B.), and NIH grants P01 GM33205 and P01 NS44232 (M.R.).

Supporting Online Material

www.sciencemag.org/cgi/content/full/304/5676/1503/DC1
Materials and Methods
SOM Text
Figs. S1 to S3
Table S1
References

19 February 2004; accepted 3 May 2004

Crystal Structure of the Long-Chain Fatty Acid Transporter FadL

Bert van den Berg,[1]* Paul N. Black,[2] William M. Clemons Jr.,[1] Tom A. Rapoport[1]

The mechanisms by which hydrophobic molecules, such as long-chain fatty acids, enter cells are poorly understood. In Gram-negative bacteria, the lipopolysaccharide layer in the outer membrane is an efficient barrier for fatty acids and aromatic hydrocarbons destined for biodegradation. We report crystal structures of the long-chain fatty acid transporter FadL from *Escherichia coli* at 2.6 and 2.8 angstrom resolution. FadL forms a 14-stranded β barrel that is occluded by a central hatch domain. The structures suggest that hydrophobic compounds bind to multiple sites in FadL and use a transport mechanism that involves spontaneous conformational changes in the hatch.

Fatty acids serve a number of essential and regulatory functions (*1*–*5*) and can be taken up by many cells from their environment. Because of their amphipathic character, they could cross membranes spontaneously, but many cells have evolved high-efficiency and regulated transport systems. In both eukaryotes and prokaryotes, several proteins are involved in fatty acid transport across the plasma membrane, but their precise roles remain to be established (*6*–*10*). In Gram-negative bacteria, fatty acids also need to cross the outer membrane (OM), where the polar layer of lipopolysaccharides (LPS) in the outer leaflet forms a major barrier (*11*). After traversing the periplasmic space (*12*), fatty acids enter the plasma membrane and are activated by a membrane-associated fatty acyl-CoA synthetase and released into the cytosol (*8*).

Transport of long-chain fatty acids (LCFAs) across the OM requires the FadL protein (*13*, *14*), a member of a distinct and conserved family of OM proteins involved in the uptake of hydrophobic compounds (*15*), including aromatic hydrocarbons destined for biodegradation (*16*, *17*). To address the question of how these proteins transport their substrates, we have determined crystal structures of FadL from *E. coli*.

FadL was crystallized in two different space groups (monoclinic and hexagonal) (*18*), both of which contain two molecules in the asymmetric unit (AU). With the exception of the N terminus, the structures are very similar [average C_α root mean square deviation (RMSD) is 0.7 Å]. In the following, we describe the structure derived from the monoclinic crystals. The protein is a monomer, with a long (~50 Å) barrel composed of 14 antiparallel β strands (Fig. 1A), a number that has not been observed in structures of other OM proteins. There is no channel connecting the extracellular milieu with the periplasm. The N-terminal 42 amino acid residues of the protein form a small compact "hatch" domain, containing three short helices, which plugs the barrel (Fig. 1B). One of the helices is capped by the conserved sequence NPA, a signature sequence in aquaporins that marks the turn of a short helix inside the membrane (*19*). A feature distinctive to FadL is that the N terminus extends a substantial distance through the barrel and occupies a position at the extracellular side of the membrane (Fig. 1B). The conformation of strand S3 in FadL is also peculiar; it has a kink that points inward, disrupting the interstrand β sheet hydrogen-bonding pattern of S3 from T99 to A105 (*20*) with neighboring strands S2 and S4, resulting in a gap in the barrel wall (Fig. 1, A and B). The kink in strand S3 is stabilized by a short antiparallel β strand between N101 to G103 and the N-terminal residues F3 through L5. The hydrogen bond between F3 and G103 may play a special role, because G103 is absolutely conserved among FadL orthologs (fig. S1).

A solvent-exposed hydrophobic groove (G) is present between the two extracellular loops L3 and L4 (Fig. 1C and Fig. 2A). In the monoclinic crystals, this groove contains several continuous and unbranched stretches of electron density, assigned as C_8E_4 molecules. One of the FadL molecules in the AU contains two C_8E_4 molecules (Fig. 1C and Fig. 2A). In the other FadL molecule, only one C_8E_4 molecule is present, at a slightly different position. The groove between L3 and L4 may therefore be a low-affinity site for the initial interaction of fatty acids with FadL.

Inside the FadL barrel, a prominent hydrophobic pocket (P) lies on the extracellular side of the membrane (Fig. 1C). The extracellular entrance to the pocket is located close to one end of the hydrophobic groove between loops L3 and L4 and is solvent accessible (Fig. 2A). More than 15 hydrophobic amino acid residues contribute to the pocket, and most of them are conserved (Fig. 2B and

[1]Howard Hughes Medical Institute and Department of Cell Biology, Harvard Medical School, 240 Longwood Avenue, Boston, MA 02115, USA. [2]Center for Metabolic Disease, The Ordway Research Institute, 150 New Scotland Avenue, Albany, NY 12208, USA.

*To whom correspondence should be addressed. E-mail: lvandenberg@hms.harvard.edu